Quasistationary analysis of the contact process on annealed scale-free networks

Silvio C. Ferreira,[1,*] Ronan S. Ferreira,[1] and Romualdo Pastor-Satorras[2]
[1]*Departamento de Física, Universidade Federal de Viçosa, 36571-000, Viçosa-MG, Brazil*
[2]*Departament de Física i Enginyeria Nuclear, Universitat Politècnica de Catalunya, Campus Nord B4, E-08034 Barcelona, Spain*
(Received 25 February 2011; revised manuscript received 10 May 2011; published 20 June 2011)

We present an analysis of the quasistationary (QS) state of the contact process (CP) on annealed scale-free networks using a mapping of the CP dynamics in a one-step process and analyzing numerically and analytically the corresponding master equation. The relevant QS quantities determined via the master equation exhibit an excellent agreement with direct QS stochastic simulations of the CP. The high accuracy of the resulting data allows a probe of the strong corrections to scaling present in both the critical and supercritical regions, corrections that mask the correct finite-size scaling obtained analytically by applying an exact heterogeneous mean-field approach. Our results represent a promising starting point for a deeper understanding of the contact process and absorbing phase transitions on real (quenched) complex networks.

DOI: 10.1103/PhysRevE.83.066113 PACS number(s): 89.75.Hc, 05.70.Jk, 05.10.Gg, 64.60.an

I. INTRODUCTION

Complex network theory represents a general unifying formalism under which it is possible to understand and rationalize the intricate connectivity and interaction patterns of many natural and manmade systems. Thus, a systematic statistical analysis of large-scale datasets has unveiled the existence of apparently universal topological features, shared by a large number of different systems from the technological, social, or biological domains [1–3]. Among these characteristics, probably the most intriguing is the discovery of the apparently ubiquitous scale-free (SF) nature of the connectivity described by a probability $P(k) \sim k^{-\gamma}$ that an element (vertex) is connected to other k elements (has degree k), with a degree exponent usually in the range $2 < \gamma < 3$ [1,3]. These and other discoveries have promoted a large modeling activity, aimed at understanding the origin and nature of the observed topological features [2,3]. In recent years, the research community has also devoted a great deal of attention to the study of the dynamical processes on complex networks [4,5], which can have important implications in the understanding of real processes such as the spread of epidemics in social systems [6] or traffic in technological systems as the Internet [7] or transport infrastructures [8].

The theoretical understanding of dynamical processes on complex networks is based in the application of mean-field approaches that are essentially based in the annealed network approximation [5]. Any nonweighted network is fully characterized by its adjacency matrix a_{ij}, taking the value 1 when vertices i and j are connected by an edge, and zero otherwise. In real (*quenched*) networks, the values of the adjacency matrix are fixed and do not change with time. When a dynamical process takes place on top of such a network, one considers the network frozen, with respect to the characteristic time scale τ_D of the dynamics. Other networks, however, are dynamical objects, changing in time over a characteristic time scale τ_N. In this case, the adjacency matrix is defined only in a statistical sense, and a complete description of the network can be given in terms of its degree distribution $P(k)$ and its degree correlations $P(k|k')$ [9]. In the limit $\tau_N \ll \tau_D$, when all edges are completely reshuffled between any two dynamical time steps, the resulting network is called *annealed* [10]. Annealed networks represent an extremely important theoretical tool because mean-field predictions for dynamical processes turn out to be exact in this kind of substrate [5].

Dynamical processes with absorbing configurations constitute a subject of outstanding interest in nonequilibrium Statistical Physics [11,12] that have also found a place in network science, as representative models of practical problems ranging from epidemic spreading [13,14], infrastructure's resilience [15,16], or activated dynamics [17], to mention just a few. The simplest lattice model allowing absorbing configurations is the classical contact process (CP) [18], whose universality class and mean-field (MF) description have been discussed in the past few years [10,19–22]. In the CP defined in an arbitrary network, vertices can be in two different states, either empty or occupied. The dynamics include the spontaneous annihilation of occupied vertices, which become empty at unitary rate, and the self-catalytic occupation of an empty vertex i with rate $\lambda n_i/k_i$, where n_i is the number of occupied neighbors of i, and k_i is its degree. The model is thus characterized by a phase transition at a value of the control parameter $\lambda = \lambda_c$, separating an active from an absorbing phase devoid of active vertices. Despite its simplicity, the CP on SF networks exhibits a very complex critical behavior, even if studied in an annealed substrate [10,21,22]. This case is particularly interesting, since in annealed networks all connections are rewired at a rate much larger than the typical rates involved in the dynamical process, implying that dynamical correlations are absent [10]. In this case, the MF approach is expected to be an exact description of the problem.

The configuration in which all vertices are empty plays a very particular role, since once the system has fallen into this state, the dynamics become frozen. For this reason, these states are called absorbing and constitute a central feature in the analysis of finite-size systems, since, in this case, the single actual stationary state is the absorbing one [11]. Finite size and absorbing states must therefore be handled using suitable strategies, concomitantly with an ansatz for the finite-size scaling (FSS) [23]. A widely adopted procedure is the

*silviojr@ufv.br; on leave at Departament de Física i Enginyeria Nuclear, Universitat Politècnica de Catalunya, Barcelona, Spain.

so-called quasistationary (QS) state [24,25], in which the absorbing configuration is suitably excluded from the dynamics.

In this work, we present a study of the QS state of the CP on SF annealed networks, combining the QS numerical approach developed in Ref. [24], suitably extended to complex networks, with the theoretical analysis of an approximated one-step process derived from mean-field theory [21]. Our analysis allows us to determine the probability distribution of activity both close to the critical point and in the off-critical regime, as well as to obtain high-quality data for relevant QS quantities, such as the density of active sites or the characteristic times. This last information is used to check the finite-size scaling forms derived from mean-field theory, which turn out to be loaded with very strong corrections to scaling.

The results presented in our paper provide a deeper understanding of the nontrivial dynamics of the contact process in annealed networks. Moreover, they open the path to the extension of the QS approach to the analysis of other dynamic processes with absorbing-phase transitions taking place on more complex and/or realistic substrates such as, for example, quenched networks and small-world topologies [26], where edges are never rewired and dynamic correlations are usually present.

We have organized our paper as follows. In Sec. II, we review the necessary background for QS analysis and numerical simulations, while in Sec. III we summarize the main results of MF theory for the CP on annealed networks. A master equation approach for the QS state is developed in Sec. IV. Section V is devoted to discuss the finite-size scaling forms of the relevant QS quantities, as well as the corrections to scaling at criticality. The off-critical analysis is discussed in Sec. VI. Finally, our concluding remarks are presented in Sec. VII.

II. FINITE SIZE AND THE QUASISTATIONARY STATE

In finite systems, the absorbing state is a fixed point that can be visited even in the supercritical phase due to stochastic fluctuations. Numerical simulations of finite systems are particularly sensitive to absorbing states and therefore suitable simulation strategies are required. The standard procedure consists in restricting the averages to those runs that did not visit the absorbing configuration [11], the so-called surviving averages. From a mathematical point of view, it is useful to define the QS state that consists of the ensemble of states accessed by the original dynamical process at long times restricted to those not trapped into an absorbing one [24]. The intensive quantities in a QS ensemble must converge to the stationary ones in the thermodynamic limit. Thus, in the active phase, the lifespan grows exponentially fast with the system size and the QS state becomes identical to the stationary one. In the subcritical phase, on the other hand, the activity in the QS state corresponds only to a few [$\mathcal{O}(1)$] particles fluctuating above the absorbing state, implying a density that vanishes inversely proportional to the system size.

Formally, the QS state is related with the original one in the limit $t \to \infty$ by

$$P(\sigma,t) = P_s(t)\bar{P}(\sigma), \tag{1}$$

where $\bar{P}(\sigma)$ is the QS probability associated to the state σ and $P_s(t)$ is the survival probability, i.e., the probability that the system is active up to time t. For a one-step process, the state of the system is completely determined by the number of occupied vertices n. Letting $P_n(t)$ be the probability that the system has n particles at time t, the QS distribution $\bar{P}_n$ is given by $P_n(t) = P_s(t)\bar{P}_n$, for which the normalization $\sum_{n\geqslant 1}\bar{P}_n = 1$ applies. The probability of visiting the absorbing state is redistributed among the active configurations, proportionally to $\bar{P}_n$, which constitutes the essence of the QS state [24]. Knowledge of the QS distribution allows the computation of the standard quantities associated to this state. For example, the probability to visit the vacuum in the CP is given by $\dot{P}_0 = P_1$, independently of the network substrate. Thus, it is straightforward to show that the survival probability and the preabsorbing state are related by $dP_s/dt = -\bar{P}_1 P_s$ providing a characteristic time scale [25]

$$\tau = \frac{1}{\bar{P}_1}. \tag{2}$$

Analogously, the density of active sites in the QS state is given by

$$\bar{\rho} = \frac{1}{N}\sum_{n\geqslant 1} n\bar{P}_n. \tag{3}$$

The standard numerical procedure to simulate the QS regime based on averages over survival runs has a limited accuracy due to the very rare achievement of surviving configurations at very large times. Thus, for instance, the stationary densities are determined as a plateau at long times in the curve $\bar{\rho}(t)$ that is usually noisy and short close to or below criticality due to the limited number of independent runs computationally accessible. The previous interpretation of the QS state provides an alternative simulation strategy, in which every time the system visits the absorbing state, this configuration is replaced by an active one randomly taken from the history of the simulation [24]. For this task, a list with M active configurations is stored and constantly updated. An update consists in randomly choosing a configuration in the list and replacing it by the present active configuration with a probability p_r. After a relaxation time t_r, the QS distributions are determined during an averaging time t_a. The improved QS method has been successfully applied to accurately determine the universality class of several models with absorbing configurations [24,27,28].

III. CP IN ANNEALED NETWORKS

The network in which dynamics takes place is assumed to be annealed and therefore completely characterized by the degree distribution $P(k)$, the probability that a randomly chosen vertex has a degree k, and the degree correlation function $P(k'|k)$ defined as the conditional probability that a vertex of degree k is connected to a vertex of degree k' [9]. The number of vertices of the network is denoted by N and its maximum degree (cutoff) by k_c [29]. In an annealed framework, the MF rate equation for the density of occupied vertices in the degree class k (i.e., the probability that a vertex of degree k is occupied) is given by [21]:

$$\frac{d}{dt}\rho_k(t) = -\rho_k(t) + \lambda k[1-\rho_k(t)]\sum_{k'}\frac{P(k'|k)\rho_{k'}}{k'}. \tag{4}$$

The first term represents the spontaneous annihilation and the second one the creation inside the compartment k due to the interaction with all compartments under the hypothesis that there are no dynamical correlations. A simple linear stability analysis shows the presence of a phase transition, located at the value $\lambda_c = 1$ and independent of the degree distribution and degree correlations, separating an active from an absorbing phase with $\rho_k = 0$ [10]. Considering, in addition, uncorrelated networks with $P(k'|k) = k'P(k')/\langle k\rangle$ [2], the overall density $\rho = \sum_k \rho_k P(k)$ obeys the equation

$$\frac{d}{dt}\rho(t) = -\rho(t) + \lambda\rho\left[1 - \langle k\rangle^{-1}\sum_k kP(k)\rho_k(t)\right]. \quad (5)$$

In Ref. [21], it was realized that the low-density regime of Eq. (5) can be understood as a one-step process (biased random walk) with transition rates

$$\begin{aligned} W(n-1,n) &= n, \\ W(n+1,n) &= \lambda n\left[1 - \langle k\rangle^{-1}\sum_k kP(k)\rho_k(t)\right], \end{aligned} \quad (6)$$

where $W(m,n)$ corresponds to the transition from a state with n particles to one with m particles. The stationary state $\partial_t\rho_k = 0$ of Eq. (4) reads as

$$\bar{\rho}_k = \frac{\lambda k\bar{\rho}/\langle k\rangle}{1 + \lambda k\bar{\rho}/\langle k\rangle}. \quad (7)$$

Close to the criticality, when the density at long times is sufficiently small such that $\bar{\rho}k_c \ll 1$, Eq. (7) becomes $\bar{\rho}_k \simeq \lambda k\bar{\rho}/\langle k\rangle$. Substituting in the transition rates, the first-order approximation for the one-step process is

$$\begin{aligned} W(n-1,n) &= n, \\ W(n+1,n) &= \lambda n(1 - \lambda g n/N), \end{aligned} \quad (8)$$

in which $g = \langle k^2\rangle/\langle k\rangle^2$. Based on numerical evidences and scaling arguments, later confirmed by more rigorous means in Refs. [10,22], the authors proposed that the critical characteristic time τ and stationary density $\bar{\rho}$ scale as [21]

$$\tau \sim (N/g)^{1/2} \quad (9)$$

and

$$\bar{\rho} \sim (Ng)^{-1/2}, \quad (10)$$

respectively. For a network with degree exponent γ and a cutoff scaling with the system size as $k_c \sim N^{1/\omega}$, where ω is an arbitrary positive parameter, the factor g scales for large N as $g \sim k_c^{3-\gamma}$ for $2 < \gamma < 3$ and $g \sim$ const for $\gamma > 3$. Therefore, the critical QS density scales as $\bar{\rho} \sim N^{-\hat{\upsilon}}$, where

$$\hat{\upsilon} = \frac{1}{2} + \max\left(\frac{3-\gamma}{2\omega}, 0\right). \quad (11)$$

Similarly, the characteristic time follows $\tau \sim N^{-\hat{\alpha}}$ with exponent

$$\hat{\alpha} = \frac{1}{2} - \max\left(\frac{3-\gamma}{2\omega}, 0\right). \quad (12)$$

The MF supercritical density for an infinite system was found to vanish at criticality as $\bar{\rho} \sim \Delta^{\beta}$, where $\beta = 1/(\gamma - 2)$ [21] and $\Delta = \lambda - \lambda_c$. For finite systems, the QS density has an anomalous cutoff-dependent FSS given by [10]

$$\bar{\rho}(\Delta, N) = \frac{1}{\sqrt{gN}}G\left(\Delta\sqrt{\frac{N}{g}}\right) \text{ for } \frac{\Delta}{g} \ll \frac{\lambda\langle k\rangle}{k_c}, \quad (13)$$

where $G(x) \sim x$ for $x \gg 1$ and $G(x)$ is constant for $x \ll 1$. The anomaly lies on the supercritical density dependence on the system size through the factor g given by $\bar{\rho} \sim \Delta/g$ if $\Delta > \sqrt{g/N}$ [10].

IV. MASTER EQUATION APPROACH FOR THE QS STATE

In order to gain analytical information about the QS distribution not far away from the critical point, we can consider the one-step process approximation described by the transition rates in Eq. (6). Starting from them, it is possible to write down a master equation (ME) for the evolution of the number of particles $P_n(t)$, taking the standard form

$$\dot{P}_n = \sum_m W(n,m)P_m(t) - \sum_m W(m,n)P_n(t). \quad (14)$$

In the long time limit, we have $\dot{\rho}_k \approx 0$ and, consequently, Eq. (7) can be applied resulting in the ME

$$\dot{P}_n = (n+1)P_{n+1} + u_{n-1}P_{n-1} - (n+u_n)P_n, \quad (15)$$

with $u_n = \lambda n(1 - \Theta)$ and Θ given by

$$\Theta[\rho] = \frac{\lambda\rho}{\langle k\rangle^2}\sum_k \frac{k^2P(k)}{1 + \lambda k\rho/\langle k\rangle}. \quad (16)$$

Substituting now $P_n(t) = P_s(t)\bar{P}_n$ and using $dP_s/dt = -\bar{P}_1 P_s$ [25], the following recurrence relation is obtained

$$\bar{P}_n = \frac{1}{n}[(u_{n-1} + n - 1 - \bar{P}_1)\bar{P}_{n-1} - u_{n-2}\bar{P}_{n-2}], \quad (17)$$

where $n = 2, \ldots, N$ and $\bar{P}_0 \equiv 0$. The QS distributions are completely determined since $\bar{P}_1$, the initial condition to iterate Eq. (17), is given by the normalization $\sum_{n\geqslant 1}\bar{P}_n = 1$.

Full information of the QS distribution can be obtained from the ME by solving it numerically. A numerical recipe to iterate the recurrence relation is as follows [25]: Start with a guess for $\bar{P}_1^{(0)}$ and iterate Eq. (17) to find $\bar{P}_n^{(0)}$, $n = 2, \ldots, N$. Repeat the procedure using $\bar{P}_1^{(j+1)} = \bar{P}_1^{(j)}/\sum_n \bar{P}_n^{(j)}$ until normalization is reached. Suitable truncations can be used to speed up the numerical process and to prevent instabilities. The truncations at finite densities are justifiable, since the central limit theorem guarantees that fluctuations much larger or much smaller than the average are exponentially negligible.

In order to explore the properties of the QS state, we have performed extensive Monte Carlo simulations of the CP on annealed networks. We use a random-neighbor network (RNN) [10] with degree distribution $P(k) \sim k^{-\gamma}$, degree correlations $P(k'|k) = k'P(k')/\langle k\rangle$, a degree cut-off $k_c = N^{1/\omega}$, and a fixed minimum degree $k_0 = 2$. The single effect in increasing the minimum degree k_0 is a shift to higher densities, which does not affect the critical properties. In an annealed approach, all links are redefined between any two time steps in such a way that the neighbor of a given vertex is selected by randomly choosing a vertex of the network with a probability $k'P(k')/\langle k\rangle$. We

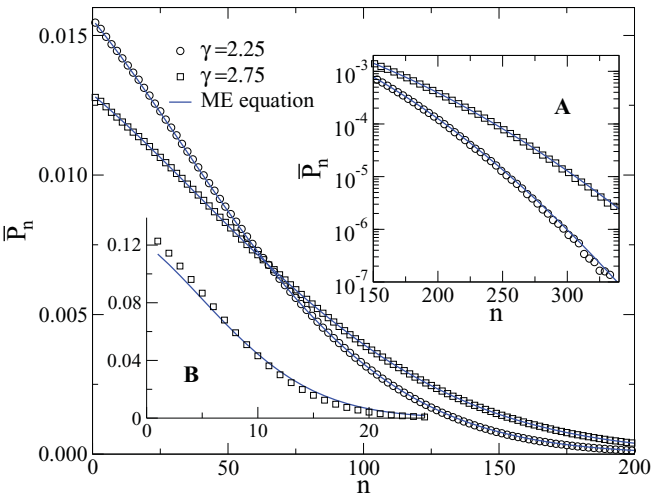

FIG. 1. (Color online) QS probability distributions at criticality obtained in simulations of the CP on annealed SF networks with a cutoff $N^{1/2}$ are compared with the numerical solutions of Eq. (17). In the main plot, the networks have size $N = 2 \times 10^4$. Inset A shows the curves of the main plot in a logarithmic scale in order to compare the tails. Inset B shows the QS distributions for a small network of size $N = 10^2$ with $\gamma = 2.75$.

perform stochastic simulations using the usual scheme [11]: At each time step, an occupied vertex is chosen at random and the time updated as $t \to t + \Delta t$, where $\Delta t = 1/[(1 + \lambda)n(t)]$ and $n(t)$ is the number of occupied vertices at time t. With probability $p = 1/(1 + \lambda)$, the occupied vertex becomes vacant. With complementary probability $1 - p = \lambda/(1 + \lambda)$, one of its neighbors (following RNN rules) is selected and, if empty, occupied. If the selected neighbor is already occupied, the simulation goes to the next step. QS states were simulated using the method described in Sec. II with $M = 10^3$, $p_r = 0.02\Delta t$, and $t_a = t_r = 10^6$. Due the short distance between vertices, the relaxation times are very short if compared with critical relaxation on regular lattices. The network sizes were varied from 10^3 to 10^7 and 50−500 network samples were used in the averages (the larger the size of the network, the smaller the number of samples). During the averaging interval, the current configuration is counted in the QS distribution with a probability proportional to its lifespan.

The QS probability distributions obtained in simulations of the critical CP are shown in Fig. 1 for different values of the degree exponent γ and network size N and compared with the results of the numerical solution of the recursion relation [Eq. (17)]. A remarkable agreement between the simulations and the one-step-process approach is achieved even for the asymptotic (Gaussian) tail as one can see in inset A of Fig. 1. A good accordance, which is improved as size increases, is observed even for sizes as small as 10^3, while neat discrepancies appears for $N \sim 10^2$ (inset B of Fig. 1). Actually, we can show that the one-step and the Langevin approach developed in Ref. [10] are equivalent in the low-density limit (see Appendix) and, consequently, the lower the density the better the one-step mapping.

V. THE QS STATE AT CRITICALITY

A. Analytical approximation at criticality

At criticality, where the densities at long times are very low, we have $u_n = \lambda n(1 - \lambda n/\Omega)$, where $\Omega = N/g$. In this limit, Eq. (15) corresponds exactly to the ME of the CP on a complete graph of size Ω, for which the QS analysis was already worked out elsewhere [25]. Analytical insights about the criticality can be obtained through a van Kampen's expansion [30] of the recurrence relation (17). Let us consider the scaling solution of Eq. (17)

$$\bar{P}_n = \frac{1}{\sqrt{\Omega}} f\left(\frac{n}{\sqrt{\Omega}}\right), \tag{18}$$

where $f(x)$ is a scaling function to be determined. Plugging Eq. (18) into (17), and performing a Taylor expansion up to second order, the result up to order Ω^{-1} is

$$x\frac{d^2 f}{dx^2} + (2 + x^2)\frac{df}{dx} + 2xf = -f_0 f, \tag{19}$$

where $f_0 = \bar{P}_1\Omega^{1/2} = f(0)$ must be chosen to impose the normalization condition $\int_0^\infty f(y)dy = 1$. Dickman and Vidgal [25] analyzed Eq. (19) numerically and checked the agreement with the recurrence relation for the CP on the complete graph. We complement the analysis by obtaining the asymptotic behaviors analytically. It is straightforward to see that the distribution decays linearly as $f(x) \simeq f_0(1 - f_0 x/2)$ for $x \ll 1$. A correction to this initial behavior can be obtained discarding the term $xf''(x)$ (a low curvature approximation) and the solution satisfying the boundary condition $f(0) = f_0$ is

$$f(x) \simeq \frac{2f_0}{2 + x^2} \exp\left[-\frac{f_0}{\sqrt{2}} \arctan\left(\frac{x}{\sqrt{2}}\right)\right], \; x \ll 1. \tag{20}$$

For $x \gg 1$, the zeroth-order terms are discarded and Eq. (19) turns to $f'' + xf' + 2f \simeq 0$. The solution satisfying the boundary condition $xf(x) \to 0$ for $x \to \infty$ ($\langle x \rangle$ is finite) is

$$f(x) \sim \exp(-x^2/2), \; x \gg 1, \tag{21}$$

implying a Gaussian tail.

In Fig. 2, we compare the results of numerical simulations of the CP at criticality ($\lambda = 1$) on a network with $N = 16 \times 10^4$ nodes, degree exponent $\gamma = 2.25$, and cutoff scaling exponent $\omega = 2$, with the corresponding analytical approximations. Despite the lack of rigor, the analytical result is in good agreement with numerical simulations. The approximation given by Eq. (20) agrees with numerical analysis, even for $x \approx 1$ or equivalently for a number of active vertices $n \approx \sqrt{\Omega}$. For the particular network of Fig. 2, we have $\sqrt{\Omega} \approx 147$. The accordance still holds for small networks ($\sim 10^3$) independently of the exponent degree and cutoff scaling.

The scaling function given by Eq. (18) encloses the FSS form of the CP at criticality. In fact, the mean number of occupied vertices at the QS regime is given by

$$\bar{n} = \sum_{n=1}^{N} n\bar{P}_n = \sum_{n=1}^{N} \frac{n}{\sqrt{\Omega}} f\left(\frac{n}{\sqrt{\Omega}}\right), \tag{22}$$

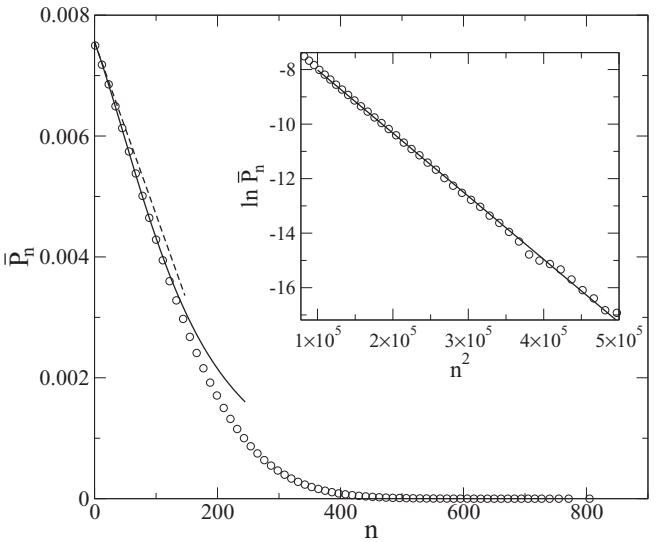

FIG. 2. Comparison between the numerical simulations of the CP on annealed networks at criticality and the asymptotic behaviors of the QS distribution given by Eqs. (20) and (21). Numerical simulations for $N = 16 \times 10^4$, $\gamma = 2.25$, and $\omega = 2$ are represented by circles and the asymptotic solutions by lines. The dashed line is the linear approximation for $n/\sqrt{\Omega} \ll 1$. The inset shows the comparison with the Gaussian tail using a straight line of slope $-1/2\Omega$.

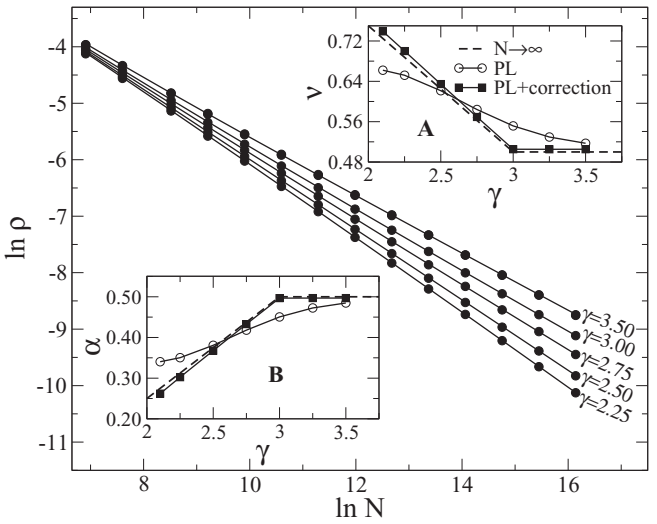

FIG. 3. QS critical density for the CP on annealed SF networks with cutoff $k_c = N^{1/2}$. In the main plot, the densities obtained with the numerical solution of the ME (lines) and QS simulations (symbols) are shown. Inset A shows the exponent of the scaling law $\bar{\rho} \sim N^{-\hat{\nu}}$, obtained analytically for asymptotically large systems ($N \to \infty$), performing a direct fit to a power-law form (PL) of the data in main figure, and performing a fit to a power with corrections to scaling. Inset B shows the same analysis for the characteristic time $\tau \sim N^{\hat{\alpha}}$.

where $\Omega = N/g$. Letting $x = n/\sqrt{\Omega}$ and $\Delta x = 1/\sqrt{\Omega}$, the sum can be approximated by a continuous integration when $N \to \infty$, namely

$$\bar{n} = \Omega^{1/2} \sum_{x=m/\sqrt{\Omega}}^{N/\sqrt{\Omega}} x f(x) \Delta x \approx \Omega^{1/2} \int_0^\infty x f(x) dx \sim \Omega^{1/2}. \tag{23}$$

Therefore, the critical QS density is simply $\bar{\rho} \equiv \bar{n}/N \sim (gN)^{-1/2}$, recovering the result first presented in Ref. [21]. Analogously, the characteristic time τ is also directly obtained by the present QS analysis by noticing that, since $\bar{P}_1 = f_0 \Omega^{-1/2}$, we have $\tau = 1/\bar{P}_1 \sim \Omega^{1/2} = (N/g)^{1/2}$.

B. Scaling at criticality

The analysis of the QS state, either by direct QS simulations or by the iterative solution of the corresponding approximate ME, allows us to obtain high-quality data for the characteristic quantities at criticality, namely the stationary density $\bar{\rho}$ and the characteristic time τ. At criticality, these quantities are expected to exhibit a scaling with system size of the form $\bar{\rho} \sim N^{-\hat{\nu}}$ and $\tau \sim N^{\hat{\alpha}}$, with exponents given by Eqs. (11) and (12) and depending on the cutoff scaling exponent ω.

QS critical densities as functions of the network size N, computed for several degree exponents and $\omega = 2$ are shown in the main plot of Fig. 3. Again, an incontestable agreement between QS simulations and the numerical ME approach is observed. Similar agreement is obtained for the analysis of the characteristic time (data not shown). However, if one tries to recover the theoretical scaling exponents, taking the values $\hat{\nu} = \max[1/2,(5-\gamma)/4]$ and $\hat{\alpha} = \min[1/2,(\gamma-1)/4]$, by means of a direct power law regression (insets in Fig. 3), a very poor agreement with the expected analytical exponents is observed, as already noted in Ref. [31]. Indeed, if we look carefully at the data we can observe that, even though a pretty good linear fit can be resolved for data range corresponding to $10^3 \leqslant N \leqslant 10^7$ as shown in Fig. 4, the actual regressions are a little bit curved. Indeed, a careful analysis of the numerical data can resolve a slight downward (negative) curvature for $\gamma \leqslant 5/2$ and an slight upward (positive) curvature for $\gamma > 5/2$ at $\lambda = \lambda_c$. In a QS analysis, these behaviors usually indicate a system slightly out of the critical point, being sub and supercritical for down and upward curvatures, respectively. But this is not the case for the data shown in Figs. 3 and 4, since the MF result is exact for the critical CP on annealed networks. Similar behaviors occur for plots of τ versus N.

As noted in [10,21], the origin of this poor agreement between theory and simulations lies in the implicit dependence on N of the g factor defining the size scaling of $\bar{\rho}$ and τ. In fact, the scaling forms $\bar{\rho} \sim N^{-\hat{\nu}}$ and $\tau \sim N^{\hat{\alpha}}$ only make sense in the limit of very large N, when g has achieved its truly asymptotic form. For intermediate values of N, instead, one should keep the scaling forms with the simultaneous dependence on g and N [21]. If we want instead to make explicit the scaling with network size, we must consider that $g = \langle k^2 \rangle / \langle k \rangle^2$ behaves, in the continuous degree limit, as

$$g = \frac{(\gamma-2)^2 k_0^{\gamma-1}}{(\gamma-1)(3-\gamma)} \frac{(1-\xi^{\gamma-1})(1-\xi^{3-\gamma})}{(1-\xi^{\gamma-2})^2} k_c^{3-\gamma}, \tag{24}$$

where $\xi = k_0/k_c < 1$. So, when $N \to \infty$, $g \sim N^{(3-\gamma)/\omega}$ for $2 < \gamma < 3$, and $g \sim$ const for $\gamma > 3$.

From Eq. (24), it is possible to work out the explicit form of the corrections to scaling in a direct analysis of the QS quantities as functions of the network size. So, considering

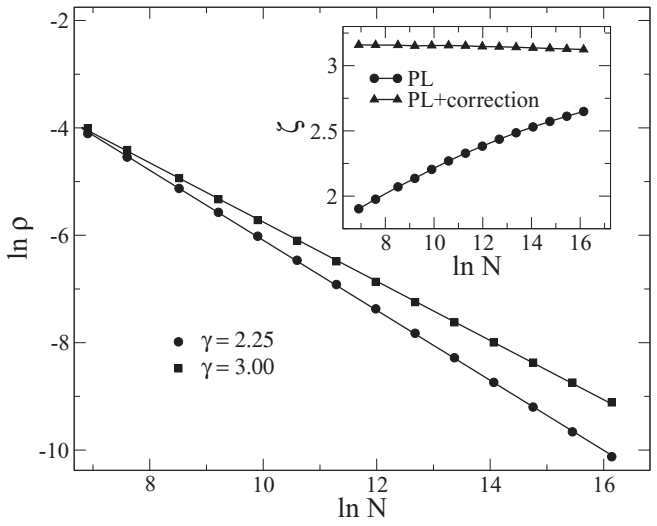

FIG. 4. Power law regressions (solid lines) of the critical QS densities (symbols) for CP on annealed SF networks with cutoff $k_c = N^{1/2}$ and degree exponents $\gamma = 2.25$ and $\gamma = 3.00$. Inset shows the QS densities for $\gamma = 2.25$ rescaled by pure power law (PL), $\zeta = \bar{\rho} N^{0.6875}$, and a PL with correction to scaling, $\zeta = \bar{\rho} N^{0.6875}(1 + 2 \times 2^{0.25} N^{-0.125} + 3 \times 2^{0.5} N^{-0.25})^{0.5}$.

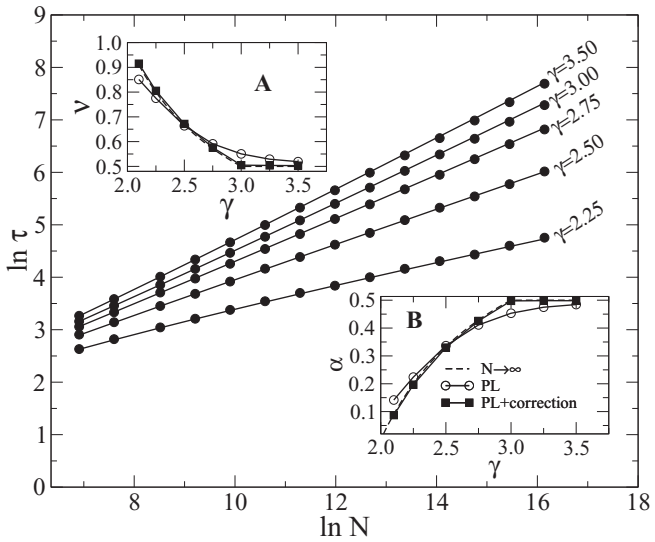

FIG. 5. Critical QS characteristic times for CP on annealed SF networks with cutoff $k_c = N^{1/(\gamma-1)}$. In the main plot, lines represent numerical solution of the ME and symbols QS simulations. The inset A shows the exponent of the scaling law $\bar{\rho} \sim N^{-\hat{\nu}}$ while the inset B shows the exponent of the scaling law $\tau \sim N^{\hat{\alpha}}$. Legends as in Fig. 3.

$2 < \gamma < 3$ and performing an expansion to leading order in ξ, Eq. (24) yields

$$g \simeq \text{const} \times (1 - \xi^{3-\gamma} + 2\xi^{\gamma-2} \cdots) k_c^{3-\gamma}. \tag{25}$$

Substituting into the MF scaling result $\bar{\rho} \sim (gN)^{-1/2}$, we obtain the expression for the stationary density

$$\ln \rho = C - \hat{\nu} \ln N + \frac{1}{2} \frac{k_0^{3-\gamma}}{N^{\frac{3-\gamma}{\omega}}} - \frac{k_0^{\gamma-2}}{N^{\frac{\gamma-2}{\omega}}}. \tag{26}$$

Notice that the corrections do not introduce any parameters to be fitted. Similar expressions are found for $\gamma \geqslant 3$. Equation (26) explains the deviations from the power law regime $\bar{\rho} \propto N^{-\hat{\nu}}$ observed for the CP on annealed SF networks. It is easy to see that the leading term for $2 < \gamma \leqslant 5/2$ is negative and causes a downward curvature, in the same way that the leading term for $\gamma > 5/2$ bends the curve upwardly. Even though the correction vanishes for $N \to \infty$, it may occur extremely slowly due to the small exponents involved. For $\gamma \approx 3$ and $\gamma \approx 2$, the corrections are logarithmic and are thus relevant for any finite size.

Introducing the corrections given in Eq. (26) in the form

$$\ln \rho' = \ln \rho - \left(\frac{1}{2} \frac{k_0^{3-\gamma}}{N^{\frac{3-\gamma}{\omega}}} - \frac{k_0^{\gamma-2}}{N^{\frac{\gamma-2}{\omega}}} \right) = C - \hat{\nu} \ln N \tag{27}$$

and performing a linear fit, the asymptotic exponent $\hat{\nu}$ is recovered as one can see in inset A in Fig. 3. Equivalent corrections can be easily obtained for $\ln \tau$ vs. $\ln N$, and the expected exponent $\hat{\alpha}$ is recovered as shown in inset B in Fig. 3. Additional proof of the strong finite size corrections is provided in the inset of Fig. 4, in which the critical QS density is rescaled by the predicted PL with exponent $\bar{\nu}$ and by this same PL with the correction given by Eq. (26). The first case is clearly size dependent while the second is flat. It is worth noting that the corrections are so strong for $\gamma = 2.25$ and $\omega = 2$ that keeping only the leading term $\mathcal{O}(N^{-0.125})$ was not enough to account for the deviation.

We additionally performed the analysis for $\omega = \gamma - 1$, which corresponds to the natural cutoff that emerges in the absence of a structural cutoff [5]. For the sake of simplicity, a hard cutoff was adopted such that connectivities larger than $k_c = N^{1/(\gamma-1)}$ are forbidden. For this cutoff, the scaling exponents for the critical density and characteristic time are $\hat{\nu} = \max[1/2, 1/(\gamma - 1)]$ and $\hat{\alpha} = \max[1/2, (\gamma - 2)/(\gamma - 1)]$, respectively. Exactly as in the $\omega = 2$ case, the QS analysis via ME agrees with simulations and the correct scaling exponents are obtained if corrections to the scaling are considered. Figure 5 shows the characteristic time and the insets therein show the scaling exponent analysis for $\omega = \gamma - 1$. Comparing the insets in Figs. 3 and 5, we can observe that the relative deviation between the exponents obtained using a simple and a corrected PL is smaller for the natural ($\omega = \gamma - 1$) than for the cutoff $k_c = N^{1/2}$. Indeed, Eq. (26) tells that the larger the cutoff exponent ω, the stronger the corrections to the scaling. However, even if the cutoffs are not imposed, the natural one emerges spontaneously in networks with power-law degree distributions [5]. Consequently, these corrections to the scaling may also be present in the CP and other dynamical processes in SF substrates, including the quenched case.

The previous results may have a remarkable impact in the analysis of absorbing phase transitions in complex networks. The usual QS analysis assumes a power-law dependence of the order parameters with the size at criticality. Such assumption is commonly used as a criterion to determine the critical point of absorbing phase transitions in regular lattices [11] and has been extended to quenched complex networks [19,20]. Corrections to scaling in the form $1 - \text{const} \times N^{-0.75}$ were already observed in QS simulations of the directed percolation

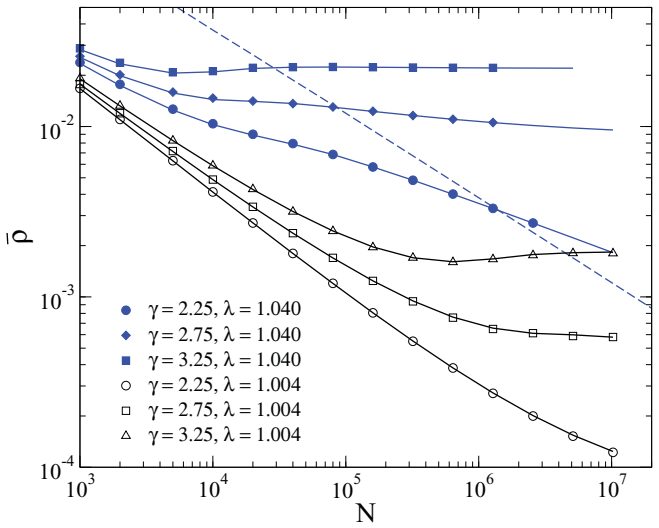

FIG. 6. (Color online) Supercritical densities as functions of the system size for three degree distributions and a cutoff $k_c = N^{1/2}$. Solid lines are the ME numerical solutions and symbols QS simulations.

universality class in hypercubic lattices, including the contact process [24,32]. Since these corrections decay with a large exponent, they are significant only for small systems. In complex networks, the scenario is quite different since the corrections, which emerge from the intrinsic SF nature of the substrate, vanish very slowly and are important even for large systems ($N \sim 10^7$ in the present work).

VI. OFF-CRITICAL QS ANALYSIS

The analysis performed for the critical CP in the previous sections is expected to work also for the off-critical phase if the densities are still sufficiently small. In Fig. 6, we compare the QS density obtained by ME iterative solution and numerical computed for networks with different degree exponents. In the

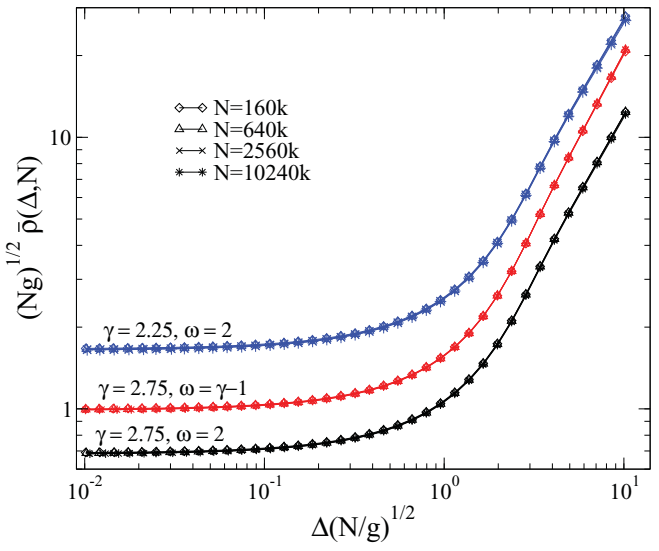

FIG. 7. (Color online) Collapses of the numerical ME solution using the anomalous scaling function given by Eq. (13). Densities obtained for network sizes $N = 16 \times 10^4$, 64×10^4, 256×10^4, and 1024×10^4 are shown. Data were shifted to avoid overlaps.

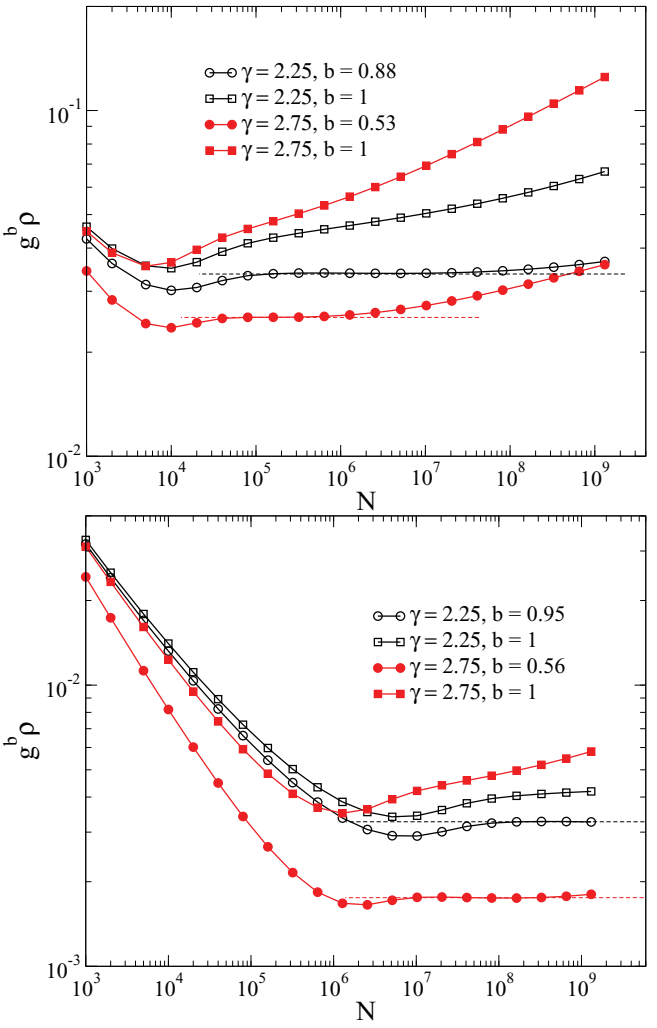

FIG. 8. (Color online) Probing the anomalous FSS $\bar{\rho} \sim \Delta/g^b$ in the ME equation iterations of the supercritical CP for $\lambda = 1.040$ (top) and 1.004 (bottom) and a cutoff exponent $\omega = 2$. Dashed horizontal lines are guides to the eye.

plot, we explore the supercritical regime with rates $\lambda = 1.004$ and 1.040 (0.4% and 4% above the critical point, respectively). The one-step ME predicts QS densities very accurately, even for a substantial distance from the critical point, corroborating that the approach is also suitable for the supercritical phase. The anomalous FSS form in the supercritical regime, Eq. (13), depending on Δ, N, and g simultaneously, is checked in Fig. 7, where we present the collapses of the data obtained from iterative solutions of the ME. Degree exponents $\gamma = 2.25$ and 2.75 using structural ($\omega = 2$) and natural ($\omega = \gamma - 1$) cutoffs are shown. Excellent collapses are obtained in all cases, in agreement with Refs. [10,22].

The strong size dependence observed in Fig. 6 for SF networks ($\gamma = 2.25$ and 2.75) but not for the homogeneous one ($\gamma = 3.25$) calls for an anomalous dependence of $\bar{\rho}$ on g, as pointed out in the Langevin [10] and random walk mapping [22] approaches. Our numerical approach allows a more detailed investigation of this issue. Inspired by the anomalous FSS prediction [10],

$$\bar{\rho} \sim \Delta/g, \Delta > \sqrt{g/N}, \tag{28}$$

we have performed a further test, analyzing the behavior of the QS density, rescaled as $g^b\bar{\rho}$, as a function of N, as shown in Fig. 8. The theoretical exponent $b = 1$, which corresponds to the anomalous scaling in Eq. (28), does not show up as a plateau in the plots of $g^b\bar{\rho}$ versus N. Interestingly, plateaus are observed if an exponent $b < 1$ is used instead. For $\lambda = 1.040$, plateaus are observed for $b = 0.88$ and $b = 0.53$ for $\gamma = 2.25$ and $\gamma = 2.75$, respectively. In an analysis performed closer to the critical point, for $\lambda = 1.004$, the plateaus are observed with larger exponents $b = 0.95$ and $b = 0.56$ for $\gamma = 2.25$ and $\gamma = 2.75$, respectively. Notice that a scaling consistent with $b = 1$ was obtained for $\gamma = 2.25$ but not for $\gamma = 2.75$. Actually, the anomalous scaling (28), derived from Eq. (13), is valid for $\sqrt{g/N} < \Delta \ll g\langle k\rangle/k_c$. For $\omega = 2$, the right and left sides of this inequality scale as $g\langle k\rangle/k_c \simeq c_\gamma N^{-(\gamma-2)/2}$ and $\sqrt{g/N} \simeq \tilde{c}_\gamma N^{-(\gamma-1)/4}$, respectively, where $c_\gamma = k_0^\gamma(\gamma-2)/(3-\gamma)$ and $\tilde{c}_\gamma^2 = k_0^{\gamma-1}(\gamma-1)(\gamma-2)^2/(3-\gamma)$ are constants of the same order and $c_\gamma > \tilde{c}_\gamma$. If γ is close to 3, the exponents involved in the lower and upper bounds of Δ are very close and we cannot make Δ sufficiently small to fulfill the upper bound and still larger than the lower one, except for numerically unaccessible large systems. Therefore, this anomalous scaling can be clearly seen only for γ close to 2. The scaling forms with $b < 1$ are thus metastable crossovers between the regimes $\bar{\rho} \sim (gN)^{-1/2}$ and $\bar{\rho} \sim \Delta/g$, that can last for decades, and could only be resolved by simulations in much larger systems sizes than those considered in this work (up to $N = 10^9$ in the ME solutions).

VII. CONCLUDING REMARKS

The contact process on scale-free networks shows remarkably rich features, even in the simple case of random annealed topologies. In the present work we have explored the quasistationary properties of this problem by combining QS numerical simulations and a master-equation approach applied to an approximate mapping to a one-step process. The resulting master equation, apart from providing quite accurate analytical approximations for the asymptotic shape of the QS activity distribution at the critical point, can be very efficiently solved numerically. The QS distribution and the relevant QS quantities (density of active sites and characteristic time) determined in this way show an excellent agreement with direct QS numerical simulations of the contact process, both at criticality and in the supercritical regime.

The high accuracy of our data has allowed us to identify strong corrections to the scaling in the critical quantities that mask the correct finite-size scaling exponents obtained analytically by means of an exact mean-field solution. Both critical density and characteristic time show tenuous curvatures as functions of the network size N due to finite-size corrections to scaling that may provide incorrect exponents if a simple power law decay is assumed. In annealed networks, for which the critical point is exactly known, we can determine the corrections to scaling analytically and thus recover the theoretical exponents in the finite-size analysis, including the abrupt change when the network loses its SF property. The analysis of the supercritical region, on the other hand, hints that those finite-size corrections are also relevant for very large network sizes. Indeed, the asymptotic scaling is observable only for extremely large values of N, much larger than those possibly attainable with present-day computers.

It is worth noticing that the QS analysis presented in this work is equivalent to the Langevin approach developed in Ref. [10] in the limit of very low densities (i.e., in the critical region; see Appendix). The main difference is that the former starts from an approximation of the original dynamical processes [Eq. (6)], while the latter represents an exact Langevin approach in the coarse-grained limit (density approximated by a continuous variable). The critical advantage of the present approach lies in the fact that our ME analysis determines the critical properties in a very intuitive way, as well as easily obtains highly accurate results, free from statistical errors, for all quantities of interest.

Our work opens the path to a more detailed characterization of absorbing phase transitions on scale-free networks, in general, and the CP in particular. In the more realistic framework of quenched networks, in which edges are frozen and do not change, this goal may be hindered by the interplay between corrections to scaling and the usual lack of knowledge about the true position of the critical point. In fact, the standard characterization of the QS state by the usual procedure assuming a simple power law of the system size at the critical point may be affected by two sources of errors: the analysis may be misleadingly done off the critical point and/or be affected by important scaling corrections. Further work in this direction, following the proposed lines, might thus help to throw light on the numerical assessment of the correct critical scaling of absorbing phase transitions on heterogeneous networks.

ACKNOWLEDGMENTS

This work was partially supported by the Brazilian agencies CNPq and FAPEMIG. S.C.F. thanks the kind hospitality at the Departament de Física i Enginyeria Nuclear/UPC. R.P.-S. acknowledges financial support from the Spanish MEC, under Project No. FIS2010-21781-C02-01; the Junta de Andalucía, under Project No. P09-FQM4682; and additional support through ICREA Academia, funded by the Generalitat de Catalunya.

APPENDIX

The connection between the Langevin approach developed in Ref. [10] and the one-step process of Eq. (6) can be established by analyzing the respective Fokker-Planck (FP) equations. The general form of a FP equation for a stochastic variable x is [30]

$$\frac{\partial P(x,t)}{\partial t} = -\frac{\partial}{\partial x}A(x)P(x,t) + \frac{\partial^2}{\partial x^2}D(x)P(x,t), \quad \text{(A1)}$$

where $A(x)$ and $D(x)$ are the drift and the diffusion terms, respectively. The Langevin analysis in Ref. [10] yielded $A(n) = n[\lambda - 1 - \lambda\Theta(n/N)]$ and $D(n) = 2\lambda n\Lambda(n/N)$, where Θ is given by Eq. (16) and

$$\Lambda(\rho) = \sum_k \frac{kP(k)}{\langle k\rangle[1+\lambda k\rho/\langle k\rangle]^3}. \quad \text{(A2)}$$

In turn, the drift and diffusion terms of the FP equation for an arbitrary one-step process is given by

$A(n) = W(n+1,n) - W(n-1,n)$ and $D(n) = W(n+1,n) + W(n-1,n)$ [30], respectively. Equation (6) results in exactly the same drift obtained in the Langevin approach, while the diffusion term takes the form $D(n) = (1+\lambda)n + \lambda\Theta(n/N)$. At low densities, one can expand Θ and Λ to leading order and obtain $D(n) \simeq 2n + \mathcal{O}(\Theta)$ in both cases. Therefore, Langevin and ME approaches are equivalent in the low-density limit.

[1] R. Albert and A.-L. Barabási, Rev. Mod. Phys. **74**, 47 (2002).

[2] S. N. Dorogovtsev and J. F. F. Mendes, *Evolution of Networks: From Biological Nets to the Internet and WWW* (Oxford University Press, Oxford, 2003).

[3] M. Newman, SIAM Rev. **45**, 167 (2003).

[4] A. Barrat, M. Barthélemy, and A. Vespignani, *Dynamical Processes on Complex Networks* (Cambridge University Press, Cambridge, 2008).

[5] S. N. Dorogovtsev, A. V. Goltsev, and J. F. F. Mendes, Rev. Mod. Phys. **80**, 1275 (2008).

[6] R. M. Anderson and R. M. May, *Infectious Diseases in Humans* (Oxford University Press, Oxford, 1992).

[7] R. Pastor-Satorras and A. Vespignani, *Evolution and Structure of the Internet: A Statistical Physics Approach* (Cambridge University Press, Cambridge, 2004).

[8] A. Barrat, M. Barthélemy, R. Pastor-Satorras, and A. Vespignani, Proc. Natl. Acad. Sci. U.S.A. **101**, 3747 (2004).

[9] M. Boguñá and R. Pastor-Satorras, Phys. Rev. E **66**, 047104 (2002).

[10] M. Boguñá, C. Castellano, and R. Pastor-Satorras, Phys. Rev. E **79**, 036110 (2009).

[11] J. Marro and R. Dickman, *Nonequilibrium Phase Transitions in Lattice Models* (Cambridge University Press, Cambridge, 1999).

[12] M. Henkel, H. Hinrichsen, and S. Lübeck, *Non-equilibrium Phase Transition: Absorbing Phase Transitions* (Springer Verlag, Netherlands, 2008).

[13] R. Pastor-Satorras and A. Vespignani, Phys. Rev. Lett. **86**, 3200 (2001).

[14] C. Castellano and R. Pastor-Satorras, Phys. Rev. Lett. **105**, 218701 (2010).

[15] D. S. Callaway, M. E. J. Newman, S. H. Strogatz, and D. J. Watts, Phys. Rev. Lett. **85**, 5468 (2000).

[16] R. Cohen, K. Erez, D. ben-Avraham, and S. Havlin, Phys. Rev. Lett. **85**, 4626 (2000).

[17] K. I. Goh, D.-S. Lee, B. Kahng, and D. Kim, Phys. Rev. Lett. **91**, 148701 (2003).

[18] T. E. Harris, Ann. Probab. **2**, 969 (1974).

[19] C. Castellano and R. Pastor-Satorras, Phys. Rev. Lett. **96**, 038701 (2006).

[20] H. Hong, M. Ha, and H. Park, Phys. Rev. Lett. **98**, 258701 (2007).

[21] C. Castellano and R. Pastor-Satorras, Phys. Rev. Lett. **100**, 148701 (2008).

[22] J. D. Noh and H. Park, Phys. Rev. E **79**, 056115 (2009).

[23] J. L. Cardy, ed., *Finite Size Scaling*, Vol. 2 (North Holland, Amsterdam, 1988).

[24] M. M. de Oliveira and R. Dickman, Phys. Rev. E **71**, 016129 (2005).

[25] R. Dickman and R. Vidigal, J. Phys. A **35**, 1147 (2002).

[26] D. J. Watts and S. H. Strogatz, Nature (London) **393**, 440 (1998).

[27] R. Dickman, Phys. Rev. E **73**, 036131 (2006).

[28] M. M. de Oliveira, S. G. Alves, S. C. Ferreira, and R. Dickman, Phys. Rev. E **78**, 031133 (2008).

[29] M. Boguñá, R. Pastor-Satorras, and A. Vespignani, Eur. Phys. J. B **38**, 205 (2004).

[30] N. G. van Kampen, *Stochastic Processes in Chemistry and Physics* (North Holland, Amsterdam, 1981).

[31] C. Castellano and R. Pastor-Satorras, Phys. Rev. Lett. **98**, 029802 (2007).

[32] R. S. Sander, M. M. de Oliveira, and S. C. Ferreira, J. Stat. Mech. Theor. Exp. (2009) P08011.